

Article

Development and Analysis of the Physicochemical and Mechanical Properties of Diorite-Reinforced Epoxy Composites

Amirbek Bekeshev ¹, Anton Mostovoy ^{2,*} , Yulia Kadykova ³, Marzhan Akhmetova ⁴, Lyazzat Tastanova ⁵ 
and Marina Lopukhova ⁶

- ¹ Laboratory “Polymer Composites”, K. Zhubanov Aktobe Regional State University, Aliya Moldagulova Avenue 34, Aktobe 030000, Kazakhstan; amirbek2401@gmail.com
- ² Laboratory “Modern Methods of Research of Functional Materials and Systems”, Yuri Gagarin State Technical University of Saratov, Polytechnichskaya St., 77, 410054 Saratov, Russia
- ³ Department “Electricity and electrical engineering”, Yuri Gagarin State Technical University of Saratov, Polytechnichskaya St., 77, 410054 Saratov, Russia; Kadykova06@yandex.ru
- ⁴ Department “Physics”, K. Zhubanov Aktobe Regional State University, Aliya Moldagulova Avenue 34, Aktobe 030000, Kazakhstan; majiko.a@gmail.com
- ⁵ Department “Chemistry and chemical technology”, K. Zhubanov Aktobe Regional State University, Aliya Moldagulova Avenue 34, Aktobe 030000, Kazakhstan; lyazzatt@mail.ru
- ⁶ Department “Economics and Humanitarian Sciences”, Yuri Gagarin State Technical University of Saratov, Polytechnichskaya St., 77, 410054 Saratov, Russia; mlopukhova@yandex.ru
- * Correspondence: Mostovoy19@rambler.ru; Tel.: +7-905-368-53-72



Citation: Bekeshev, A.; Mostovoy, A.; Kadykova, Y.; Akhmetova, M.; Tastanova, L.; Lopukhova, M. Development and Analysis of the Physicochemical and Mechanical Properties of Diorite-Reinforced Epoxy Composites. *Polymers* **2021**, *13*, 2421. <https://doi.org/10.3390/polym13152421>

Academic Editor: Yung-Sheng Yen

Received: 7 July 2021

Accepted: 21 July 2021

Published: 23 July 2021

Publisher’s Note: MDPI stays neutral with regard to jurisdictional claims in published maps and institutional affiliations.



Copyright: © 2021 by the authors. Licensee MDPI, Basel, Switzerland. This article is an open access article distributed under the terms and conditions of the Creative Commons Attribution (CC BY) license (<https://creativecommons.org/licenses/by/4.0/>).

Abstract: The aim of this paper is to study the effect of a polyfunctional modifier oligo (resorcinol phenyl phosphate) with terminal phenyl groups and a dispersed mineral filler, diorite, on the physicochemical and deformation-strength properties of epoxy-based composites. The efficiency of using diorite as an active filler of an epoxy polymer, ensuring an increase in strength and a change in the physicochemical properties of epoxy composites, has been proven. We selected the optimal content of diorite both as a structuring additive and as a filler in the composition of the epoxy composite (0.1 and 50 parts by mass), at which diorite reinforces the epoxy composite. It has been found that the addition of diorite into the epoxy composite results in an increase in the Vicat heat resistance from 132 to 140–188 °C and increases the thermal stability of the epoxy composite, which is observed in a shift of the initial destruction temperature to higher temperatures. Furthermore, during the thermal destruction of the composite, the yield of carbonized structures increases (from 54 to 70–77% of the mass), preventing the release of volatile pyrolysis products into the gas phase, which leads to a decrease in the flammability of the epoxy composite. The efficiency of the functionalization of the diorite surface with APTES has been proven, which ensures chemical interaction at the polymer matrix/filler interface and also prevents the aggregation of diorite particles, which, in general, provides an increase in the strength characteristics of epoxy-based composite materials by 10–48%.

Keywords: epoxy oligomer; modification; plasticizer; filler; diorite; physicochemical and mechanical properties

1. Introduction

In the modern world, requirements for performance properties for various materials and products obtained from them are constantly increasing and it is possible to provide them by selecting raw materials and the technological parameters of production [1–3].

The combining or physicochemical modification of various materials that make up epoxy compositions makes it possible to directly control the most important properties of epoxy composites. The addition of plasticizers provides the elasticity of polymeric materials and can change their glass transition temperature [3–5]. The addition of fillers ensures an increase in the strength of epoxy composites and imparts specific physical and

chemical properties to them [6–9]. The effect of the addition of a filler on the properties of the polymer is determined by many factors: the chemical nature of the polymer and filler, the nature of the filler surface, the size and shape of its particles, the ability to form their own structures, a change in the conformational set of macromolecules and the structure of the polymer itself. The added fillers with different quantitative content have different effects on the structure of polymers [10–13].

It was shown in the work [14,15] that the integration of silica nanoparticles in an epoxy nanocomposite can greatly improve the mechanical properties of the resultant composite materials, including, but not limited to, tensile strength, fracture toughness, impact and fatigue properties.

The authors of [16,17] propose to use technogenic waste from industrial enterprises—fly ash, which is a by-product of coal burning at thermal power plants—as a filler for epoxy composites. Fly ash was introduced into the epoxy composite in an amount of 10–50 vol.%. The studies carried out have shown that, as the amount of fly ash increases to the critical point (30 vol.%), an increase in tensile strength is apparent, while the compressive strength of the composite continuously increases with an increase in the fly ash content. In addition, it was found that reducing the particle size of fly ash provides the production of epoxy composites with higher physical and mechanical properties.

In work [18], bi-functionalized montmorillonite was used as a filler in epoxy composites. Epoxy composites filled with organoclay have higher thermal stability; in addition, the introduction of organoclay provides an increase in the yield of carbonized structures being a physical barrier for the interdiffusion of the oxidizer and combustible gases into the combustion zone, which reduces the flammability of the epoxy composite. Studies have shown that the optimal amount of bi-functionalized montmorillonite is 1 wt.%, which provides an increase in storage modulus, cross-link density and glass transition temperature of epoxy composite.

Granite powder is a promising filler for epoxy composites, the introduction of which not only reduces the cost of composites but also improves their physical and mechanical properties. In work [19], to increase the adhesive interaction at the polymer matrix/filler interface, the granite powder was treated with triethoxymethylsilane. Granite powder was added to the epoxy composition in an amount of 0–60 wt.%. Composites with 50 wt.% of granite powder were found to have maximum mechanical properties in all cases. The treatment of granite powder with a silane coupling agent improves the mechanical properties of epoxy composites based on it and also improves the interfacial bond between the granite powder and the epoxy matrix.

The study of the mechanism of physical and chemical cross-linking processes when various plasticizers and fillers are added into an epoxy binder is an important issue in modern materials science.

Currently, despite a large number of works devoted to the study of the effect of various fillers and plasticizers, there are still insufficiently studied issues related to their influence on the processes of structure formation and the structure and performance characteristics of polymer composite materials, which predetermines the direction of research in this work.

The aim of this paper is to study the effect of a polyfunctional modifier oligo (resorcinol phenyl phosphate) with terminal phenyl groups and a dispersed mineral filler, diorite, on the physicochemical and deformation-strength properties of epoxy-based composites.

2. Materials and Methods

2.1. Materials

We used ED-20 epoxy resin (GOST 10587-93) manufactured by CHIMEX Limited (St. Petersburg, Russia) as a binder for the preparation of polymer composite materials, and polyethylene polyamine (PEPA) (TU 6-02-594-85) manufactured by CHIMEX Limited (St. Petersburg, Russia) as a hardener.

Oligo (resorcinol phenyl phosphate) with terminal phenyl groups Fyrolflex (ORPP) manufactured by ICL Industrial Products America Inc. (New York City, NY, USA) was used as a plasticizer and flame retardant.

ORPP is an oligomeric halogen-free plasticizer with flame-retardant properties. Compared to other halogen-free (phosphate) fire retardants, it has low volatility and stability (onset of thermal degradation at +370 °C), which allows its use for modifying most technical plastics. The advantage of ORPP over other bis-phosphates is its lower viscosity, which makes the product easier to handle and improves its technological properties (lower mixing temperature) [6,20].

Table 1 shows the typical properties and specifications of epoxy resin, hardener and ORPP.

Table 1. Typical properties and specifications of epoxy resin, hardener and ORPP.

The Qualitative Characteristics	Value
Properties of epoxy resin ED-20	
Content of epoxy groups, %	20.0–22.5
Viscosity, Pa × s	13–20
Epoxy equivalent, g/mol	195–216
Density at 25 °C, kg/m ³	1166
Properties of PEPA	
Molecular mass, g/mol	230–250
Viscosity, Pa × s	0.6–0.9
Density at 25 °C, kg/m ³	1020
Amine number, mg KOH/g	1250
Nitrogen content, % by weight	30.0
Properties of ORPP	
Viscosity, Pa × s	0.4–0.6
Density at 25 °C, kg/m ³	1250–1295
Phosphorus content, % by weight	10.6–10.8
Acidity, mg KOH/g	0.10–0.12
Boiling temperature, °C	≥300
Decomposition temperature, °C	370

The presence of phosphorus (10.7%) as a combustion inhibitor in ORPP ensures the structuring of the epoxy composite when exposed to elevated temperatures, which leads to an increase in the yield of carbonized structures being a physical barrier for the interdiffusion of the oxidizer and combustible gases into the combustion zone, which reduces the flammability of the epoxy composite [6,20,21].

As a filler for epoxy composites, we used finely ground magmatic plutonic rock, diorite, from the Priorskoye deposit (Novorossiysk district of Aktobe region, Kazakhstan). The choice of diorite as a filler for polymer composites is due to its availability; diorite is very actively mined in Chile, Peru, Ecuador, Sweden and Norway. In Kazakhstan and Russia, there are several very large deposits of this rock. In addition, diorite is not only hard, but also viscous, which ensures high wear resistance of the rock. The choice of diorite as a filler is associated not only with its availability but also with a certain chemical composition: the presence of metal oxides (iron oxides, calcium, aluminum and titanium) will allow diorite to be used as a flame retardant for epoxy polymers. Based on the properties of diorite, it can be expected that its introduction into a polymer composition will provide an increase in the physicochemical and mechanical properties of polymer composites.

2.2. Functionalization of the Diorite Surface

The diorite surface was functionalized with γ -aminopropyltriethoxysilane (APTES) manufactured by Penta-91 (Russia). For this, 0.5 g of diorite was dispersed in 100 ml of a solution of H₂O—APTES (95–5) for 10 min using an ultrasonic homogenizer. To increase the solubility of APTES in water, the pH of the mixture was brought to 5 with the gradual addition of acetic acid. We selected an acidic media (CH₃COOH) in order to increase the level of silanol formation and to decrease self-condensation reactions between the hydro-lyzed silanol groups. To remove the remaining silane compound around the diorite particles, the resulting suspension was centrifuged and washed twice with H₂O [22]. Then the product was dried at 105 °C in the laboratory oven for 5 h.

2.3. Characterization of Diorite

The surface morphology of the samples was studied using a Tescan VEGA 3 SBH scanning electron microscope (Brno, Czech Republic). X-ray phase analysis was carried out using an ARL X'TRA diffractometer (CuK α radiation, $\lambda = 0.15412$ nm, angle range 2θ 5°–60°). The diffraction patterns were interpreted using the Powder Diffraction File-2 (PDF-2) database of the International Center for Diffraction Data (ICDD) and the Crystallographic Search-Match program, version 3.1.0.2.B. The chemical composition of diorite was determined on an X-ray analytical microprobe-microscope PAM 30- μ . FT-IR spectroscopy was carried out using the Shimadzu IRTracer-100.

The size distribution of diorite particles was determined by laser diffraction in an aqueous medium using a Fritsch Analysette-22 Nanotech analyzer (Fritsch, Germany) in the range of 0.01–1000 μ m. Determination of the specific surface area of the samples was carried out using an Quantachrome Nova 2200 surface area and porosity analyzer from the low-temperature nitrogen adsorption.

2.4. Preparation of Epoxy Composites

Diorite was added into the plasticized ORPP epoxy composition as a modifying additive (0.05–0.50 parts by mass) and a filler (50–100 parts by mass). For uniform distribution of the filler in the polymer matrix and preventing its aggregation, ultrasound treatment of the epoxy composition was used (ultrasound exposure parameters: frequency 22 ± 2 kHz, duration 60 min) [6].

The epoxy composition was cured at room temperature for 24 ± 1 h, followed by stepwise heat treatment at 90 ± 5 °C for 2 h and at 120 ± 5 °C for 2 h [6,13,20].

2.5. Testing of the Composites

Tests of samples for resistance to tensile and bending loads were carried out on a WDW-5E universal electromechanical testing machine from Time Group Inc., Beijing, China, at a test speed of 5 mm/min for the tensile test and 50 mm/min for the bending test. The bending stress and flexural modulus was determined according to ISO 178: 2019; the tests were carried out on samples in the form of blocks with 4 mm thickness, 10 mm width and a working-part length of 80 mm. The strength and modulus of tensile elasticity was determined according to ISO 527-2: 2012; the tests were carried out on samples in the form of spatulas with 4 mm thickness, 10 mm width and a working-part length of 50 mm.

Compressive strength was determined in accordance with ISO 604: 2002; the tests were carried out on samples in the form of a cube with rib length 30 mm. The impact strength was determined in accordance with ISO 179-1: 2010 using an LCT-50D pendulum impact machine (Beijing United Test Co., Ltd., Beijing, China); the tests were carried out on samples in the form of blocks with 4 mm thickness, 10 mm width and a working-part length of 80 mm.

The Brinell hardness was determined in accordance with ISO 2039-1: 2001 using an HBE-3000A electronic Brinell hardness tester (Beijing United Test Co., Ltd., Beijing, China). The determination of the Vicat heat resistance was carried out according to ISO 306: 2013, method B50–load 50 N; temperature rise rate 50 °C/h.

The surface morphology of the samples was studied using a Tescan VEGA 3 SBH scanning electron microscope (Brno, Czech Republic).

Thermal stability of the samples was determined by a thermogravimetric analysis using a Q-1500D derivatograph (MOM, Budapest, Hungary) of the Paulik–Paulik–Erdey system under the following experimental conditions: weighed portion—100 mg, medium-air, heating interval—up to 1000 °C, heating rate -10 °C/min, a relative error that does not exceed 1%.

To determine the mass loss during ignition in air, samples were made with a width 35 ± 1 mm, a length 150 ± 3 mm and a height 4 ± 1 mm. Pre-weighed (accurate to 0.0001 g) samples were suspended vertically in the center of a metal tube so that the end of the sample protruded 5 mm and was 10 mm above the gas burner. A gas burner with a flame height of 40 ± 5 mm was placed under the sample in its center. After 2 min of exposure to the flame, the ignition source was removed, and the sample continued to burn or smolder on its own. After cooling to room temperature, the sample was weighed (with an accuracy of 0.0001 g), and the weight loss was determined as a percentage of the initial sample weight using the formula: $\Delta m = (m_1 - m_2) \cdot 100 / m_1$, where m_1 —sample weight before testing; m_2 —sample weight after testing.

The self-heating temperature of the sample during the curing of the epoxy composition was determined according to the method described in [7].

The degree of curing of epoxy composites was determined by extracting samples of the crushed material with acetone in a Soxhlet apparatus. A sample of finely ground material weighing 1 g was poured with 20 ml of acetone and extracted in the apparatus for 24 h., then the material was dried and the dry residue was weighed with an accuracy of 0.0001 g. The change in weight was calculated by the formula: $\Delta m = (m_1 - m_2) \cdot 100 / m_1$, where m_1 —initial sample weight; m_2 —weight of the sample after extraction and drying. The degree of curing (X) was determined by the formula: $X = 100 - \Delta m$.

3. Results and Discussion

According to SEM data, diorite crystals are flattened, tabular to scaly or lamellar, Figure 1.

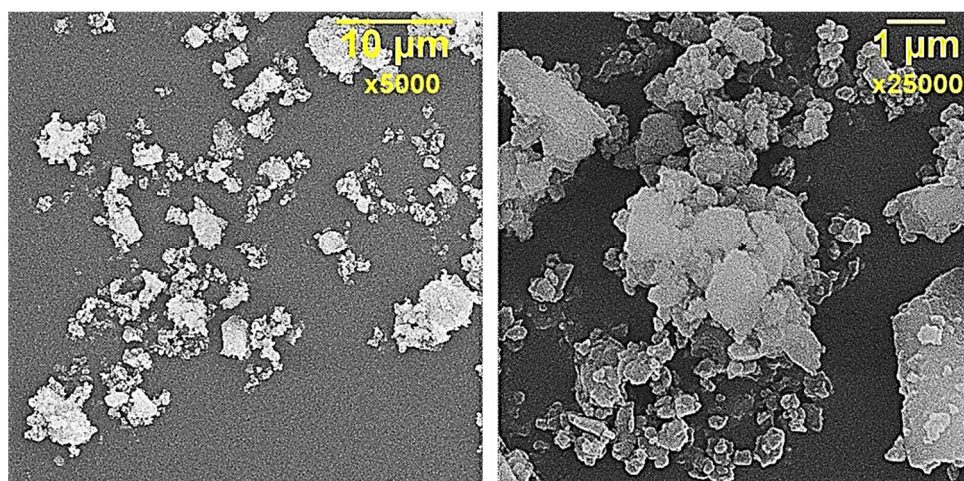


Figure 1. SEM of diorite particles.

The study of the chemical composition of diorite has shown that it mainly consists of iron oxides, silicon, calcium, aluminum and titanium, Table 2.

The fractional composition of diorite is represented by particles from 0.2 to 50 µm, with average particle sizes of 1–2 and 20–25 µm, Figure 2.

XRF data have shown that diorite is represented by four different phase structures, in Figure 3.

Table 2. Chemical composition of diorite.

Component	Concentration, %
Fe ₂ O ₃	41.2
SiO ₂	22.9
CaO	20.3
Al ₂ O ₃	10.8
TiO ₂	2.4
CuO	1.2
Mn ₂ O ₇	0.7
K ₂ O	0.3
P	0.1
S	0.06

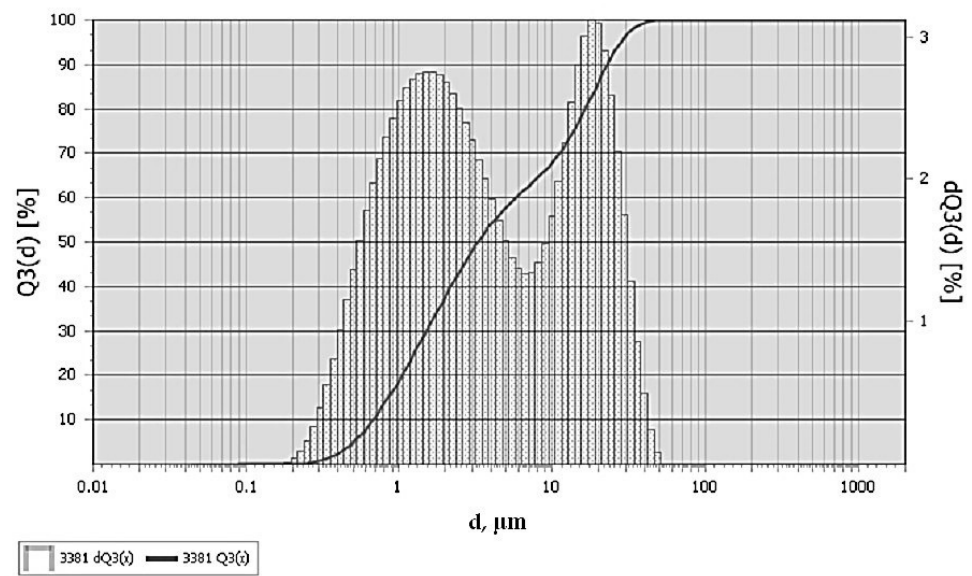


Figure 2. Fractional composition of diorite.

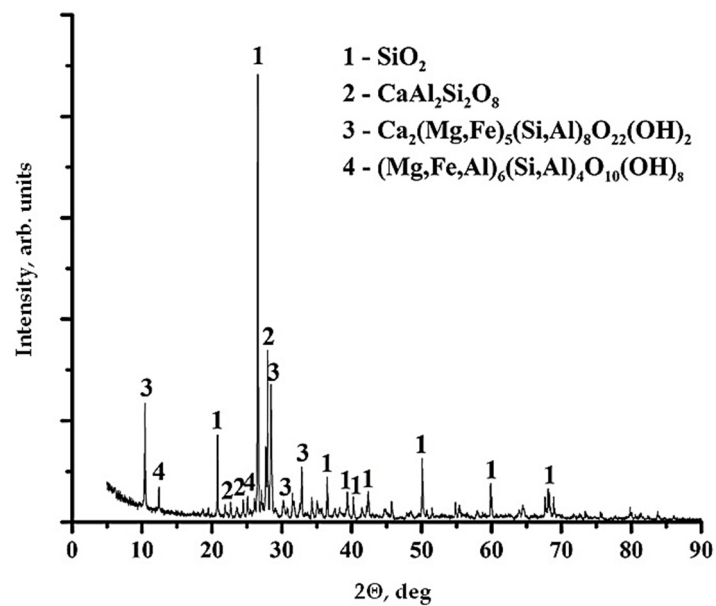


Figure 3. XRF data for diorite.

The specific surface area of diorite particles, determined using a Quantachrome Nova 2200 Surface Area and Pore Size Analyzer by a low-temperature nitrogen adsorption method, is 5.6 m²/g.

Thus, the analysis of the structure and specific surface area of diorite has shown that it can be used as a structuring additive and filler for epoxy composites, which should ensure an increase in their performance properties. Pre-drying the filler is not required because the moisture content in diorite is 0.4%.

Based on results of the studies, it has been found that the optimal content of diorite as a structuring additive in the epoxy composition is 0.1 parts by mass, which provides a significant increase in the indicators of physical and mechanical properties: the bending stress increases by 19%; the compressive strength increases by 15%; the strength increases by 80%, and the tensile modulus increases by 31%; the impact strength increases by 100%; the Brinell hardness increases by 20%; all are shown in Table 3.

Table 3. Properties of epoxy composites.

Composition, Parts by Mass, Cured by 15 Parts by Mass of PEPA	σ_{ben} , MPa	E_{ben} , MPa	σ_{com} , MPa	σ_{ten} , MPa	E_{ten} , MPa	a_{im} , kJ/m ²	H_b , MPa	H_v , MPa
100ED-20 + 40 ORPP	80 ± 3.2	2210 ± 88	100 ± 4.0	30 ± 1.5	1896 ± 94	6 ± 0.3	175 ± 10	174 ± 10
100 ED-20 + 40 ORPP + 0.05 Diorite	82 ± 3.3	2255 ± 90	105 ± 4.2	40 ± 1.8	2115 ± 105	7 ± 0.4	185 ± 11	184 ± 11
100 ED-20 + 40 ORPP + 0.1 Diorite	95 ± 3.8	2343 ± 92	115 ± 4.5	54 ± 2.4	2490 ± 120	12 ± 0.7	210 ± 12	209 ± 12
100 ED-20 + 40 ORPP + 0.5 Diorite	90 ± 3.5	2506 ± 98	120 ± 4.8	41 ± 1.8	2952 ± 142	7 ± 0.4	240 ± 14	240 ± 14
100 ED-20 + 40 ORPP + 10 Diorite	90 ± 3.6	3556 ± 140	130 ± 5.0	40 ± 1.8	3100 ± 150	5 ± 0.2	250 ± 15	250 ± 15
100 ED-20 + 40 ORPP + 30 Diorite	95 ± 3.7	6540 ± 261	140 ± 5.2	42 ± 2.0	4110 ± 202	5 ± 0.2	275 ± 16	278 ± 16
100 ED-20 + 40 ORPP + 50 Diorite	105 ± 3.9	8058 ± 322	155 ± 6.2	42 ± 2.0	4600 ± 220	5 ± 0.2	295 ± 17	299 ± 17
100 ED-20 + 40 ORPP + 75 Diorite	70 ± 2.6	8950 ± 355	150 ± 6.0	38 ± 1.5	4920 ± 245	4 ± 0.2	310 ± 18	315 ± 18
100 ED-20 + 40 ORPP + 100 Diorite	58 ± 2.1	9812 ± 389	125 ± 4.8	35 ± 1.4	5200 ± 260	4 ± 0.2	340 ± 20	351 ± 20

Note: σ_{ben} —bending stress; E_{ben} —modulus of elasticity in bending; σ_{com} —compressive strength; σ_{ten} —tensile strength; E_{ten} —tensile modulus of elasticity; a_{im} —impact strength, H_b —Brinell hardness, H_v —Vickers hardness.

The optimal content of diorite as a filler is 50 parts by mass, which not only reduces the cost but also increases the strength characteristics of filled epoxy composites: the bending stress increases by 31%, and the modulus of elasticity in bending increases by 3.6 times; the compressive strength increases by 55%; the tensile strength increases by 40%, and the tensile modulus increases by a factor of 2.4; the Brinell hardness increases by 68%, while the impact toughness remains at the level of the unfilled plasticized composite, as shown in Table 3.

The change in the viscosity of the epoxy composition when diorite is introduced into it is shown in Table 4.

Table 4. Viscosity of epoxy compositions at 25 °C.

Composition, Parts by Mass	Viscosity, P × s
100 ED-20 + 40 ORPP	1.50 ± 0.07
100 ED-20 + 40 ORPP + 0.05 Diorite	1.50 ± 0.07
100 ED-20 + 40 ORPP + 0.1 Diorite	1.55 ± 0.08
100 ED-20 + 40 ORPP + 0.5 Diorite	1.60 ± 0.09
100 ED-20 + 40 ORPP + 10 Diorite	3.90 ± 0.18
100 ED-20 + 40 ORPP + 30 Diorite	15.20 ± 0.65
100 ED-20 + 40 ORPP + 50 Diorite	24.50 ± 1.10
100 ED-20 + 40 ORPP + 75 Diorite	32.30 ± 1.40
100 ED-20 + 40 ORPP + 100 Diorite	40.60 ± 1.80

From the presented SEM data, it can be seen in Figure 4 that, by adding diorite, a monolithic structure of the sample is formed and an almost complete absence of aggregates of diorite particles is observed, as shown in Figure 4b. The binder molecules repeat the layer morphology of the filler, as shown in Figure 4b–c, which is apparently one of the facts explaining the significant increase in the properties of epoxy composites in the presence of an active filler, diorite.

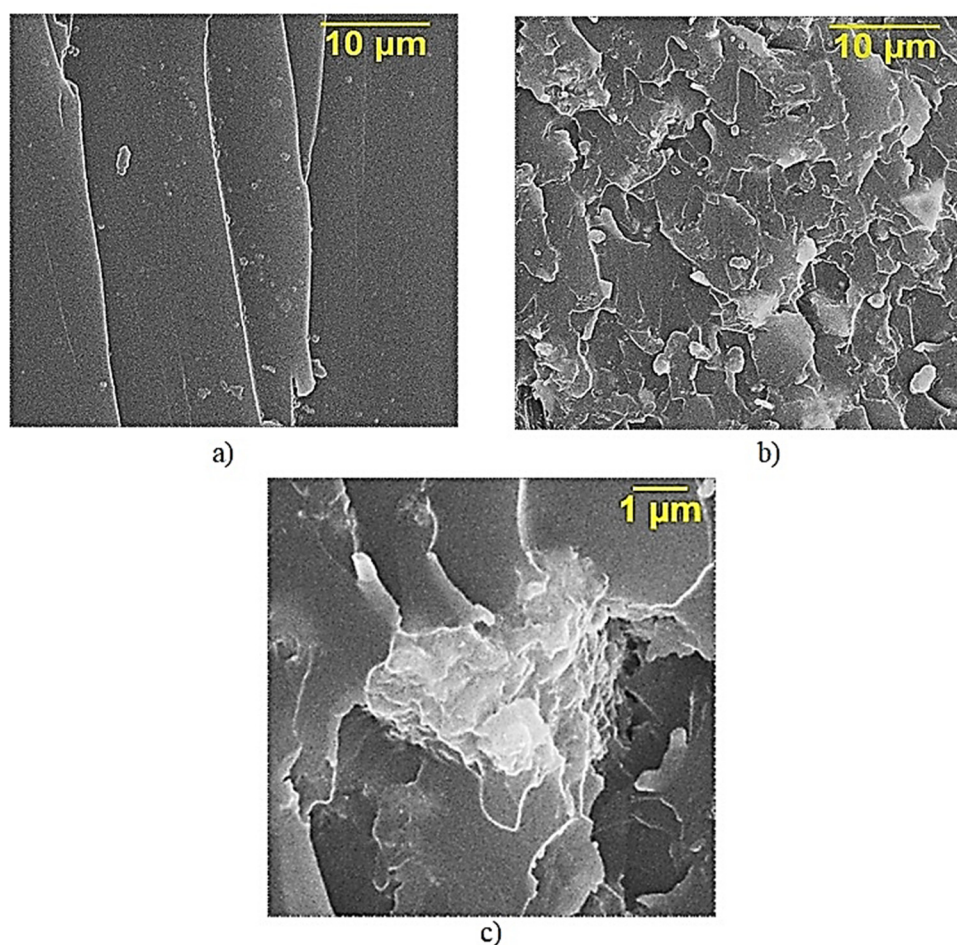


Figure 4. SEM data of samples of epoxy composites, parts by mass: (a)—100 ED-20 + 40 ORPP + 15 PEPA ($\times 5000$); (b)—100 ED-20 + 40 ORPP + 50 Diorite + 15 PEPA ($\times 5000$); (c)—100 ED-20 + 40 ORPP + 50 Diorite + 15 PEPA ($\times 25,000$).

The analysis of the literature data has shown that the addition of dispersed fillers affects the kinetic characteristics of the polymerization reaction of the epoxy composition during curing as well as the formation of the phase structure of the composite material [6,13,23–27].

The analysis of the curing kinetics of epoxy compositions has shown that the addition of diorite (0.1 parts by mass) has an initiating effect on the processes of structure formation, as shown in Figure 5, which is observed in the reduction in the gelation time from 27 to 24 min and the curing time from 38 to 34 min. However, with the addition of diorite as a filler (50 parts by mass), the gelation time and curing time slightly increase (from 27 to 29 min and from 38 to 40 min, respectively), which is apparently due to the high viscosity of the composition and steric hindrances in the curing process, as shown in Table 5.

Table 5. Values of the curing process of epoxy composites.

Composition, Parts by Mass, Cured by 15 Parts by Mass of PEPA	τ_{gel} , min	τ_{cur} , min	T_{max} , °C	X_c , %
100 ED-20 + 40 ORPP	27	38	88	90.0
100 ED-20 + 40 ORPP + 0.1 Diorite	24	34	135	94.0
100 ED-20 + 40 ORPP + 50 Diorite	29	40	116	98.0
100 ED-20 + 40 ORPP + 50 Diorite _(APTES)	19	28	122	98.6

Note: τ_{gel} —the duration of gelation process, τ_{cur} —the duration of curing, T_{max} —the maximum curing temperature, X_c —curing degree.

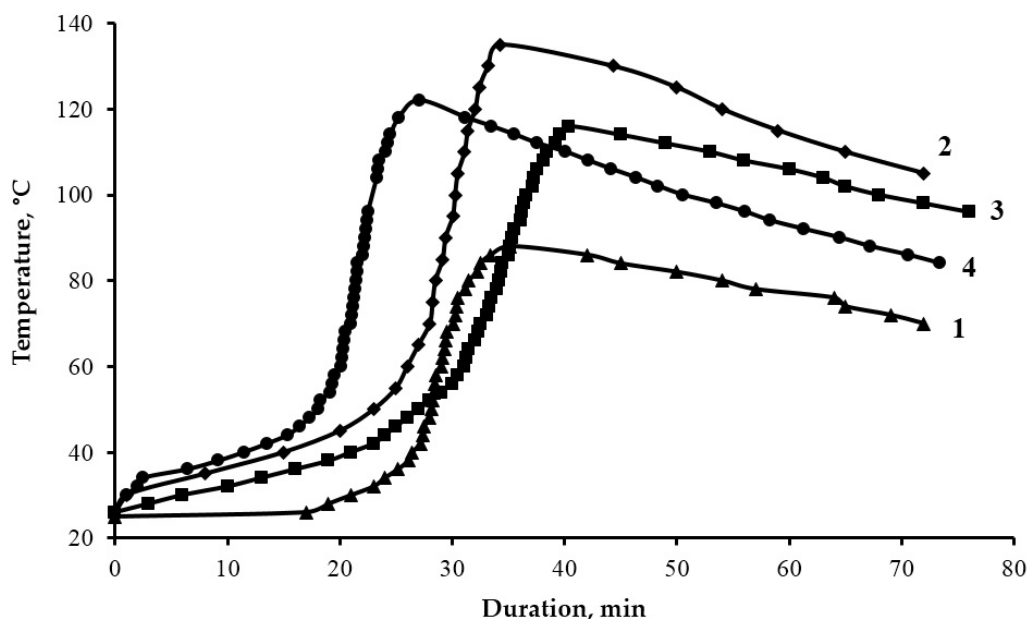


Figure 5. Kinetic curves of the curing process of epoxy composites: 1—100 ED-20 + 40 ORPP + 15 PEPA; 2—100 ED-20 + 40 ORPP + 0.1 Diorite + 15 PEPA; 3—100 ED-20 + 40 ORPP + 50 Diorite + 15 PEPA; 4—100 ED-20 + 40 ORPP + 50 Diorite_(APTES) + 15 PEPA.

Thus, in both cases, there is a significant increase in the maximum curing temperature from 88 to 116–135 °C. Besides, the addition of diorite into the epoxy composition provides an increase in the curing degree of the epoxy composite from 90 to 94–98%, which allows the assumption that the diorite particles are additional cross-linking centers.

Differential scanning calorimetry data confirmed the results obtained, as shown in Figure 6, in which the introduction of diorite into the epoxy composition provides an increase in the thermal effect of the reaction and a decrease in the temperature of the onset of curing from 46 to 33–36 °C; in addition, an increase in the glass transition temperature of the epoxy composite was noted, as shown in Table 6.

The addition of diorite into the epoxy composition provides an improvement of the physicochemical and thermophysical parameters of epoxy composites, which is observed in an increase in the Vicat heat resistance from 132 to 140–188 °C, as shown in Table 7. Besides, the thermal stability of the composite increases, which can be seen in a shift of the initial temperature of the main stage of destruction to the area of higher temperatures (from 230 to 240–245 °C). It has been found that the thermal destruction of the composite containing diorite increases the yield of carbonized structures from 54 to 70–77%, which prevents the release of volatile thermolysis products into the gas phase, thus leading to a decrease in the flammability of the epoxy composite [21], which is observed in a decrease in weight loss during ignition in air to 1.8–2.2% and an increase in the oxygen index from 28 to 30–32% by volume, as shown in Table 7. Thus, diorite-filled epoxy composites belong to the class of flame-retardant materials.

Table 6. Results of differential scanning calorimetry of epoxy compositions.

Composition, Parts by Mass, Cured by 15 Parts by Mass of PEPA	T_{start} – T_{end} T_{max} °C	T_{glass} , °C	H, J/g
100 ED-20 + 40 ORPP	46–167 108	78	415
100 ED-20 + 40 ORPP + 0.1 Diorite	36–175 110	81	893
100 ED-20 + 40 ORPP + 50 Diorite	34–211 109	84	703

Note: T_{start} , T_{end} —temperature of the start and end of the curing process, T_{max} —the temperature of the maximum heat release during curing, H—thermal effect of reaction.

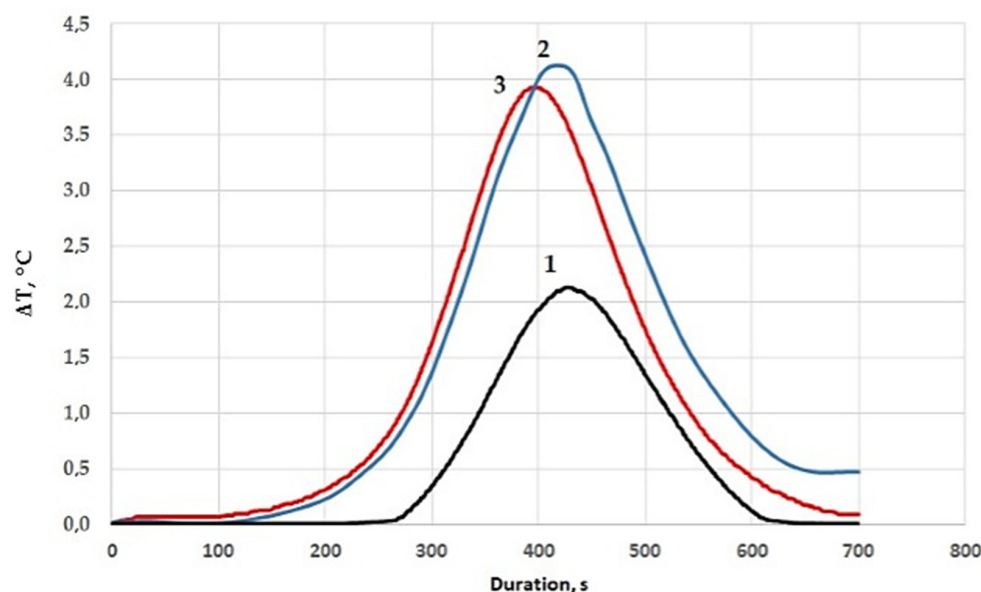


Figure 6. Differential scanning calorimetry of epoxy compositions: 1—100 ED-20 + 40 ORPP + 15 PEPA; 2—100 ED-20 + 40 ORPP + 0.1 Diorite + 15 PEPA; 3—100 ED-20 + 40 ORPP + 50 Diorite + 15 PEPA.

Table 7. Physicochemical properties of epoxy composites.

Composition, Parts by Mass, Cured by 15 Parts by Mass of PEPA	T_{in} , °C	T_f , °C	Yield of CS at T_f , % Mass	Δm , %	OI, %	T_v , °C
100 ED-20	200	390	40 (390 °C)	78	19	86
100 ED-20 + 40 ORPP	230	370	54 (370 °C)	4.7	28	132
100 ED-20 + 40 ORPP + 0.1 Diorite	240	380	56 (380 °C)	4.4	28	140
100 ED-20 + 40 ORPP + 50 Diorite	245	380	70 (380 °C)	2.2	30	180
100 ED-20 + 40 ORPP + 100 Diorite	245	370	77 (370 °C)	1.8	32	188

Note: T_{in} , T_f —initial and final temperature of the main stage of thermolysis; Δm —weight loss when ignited in air; OI—oxygen index; T_v —Vicat heat resistance.

Since epoxy resins have good adhesion to most materials [28–30], we used the developed compositions for the fire protection of wood. Wood samples with a fire-resistant coating (100 ED-20 + 40 ORFF + 50 Diorite + 15 PEPA) were obtained.

When determining the speed of flame propagation over the wood surface without a fire-resistant coating and with a fire-resistant coating, it was found that the uncoated wood ignites in 15 s and combustion continues after the gas burner is removed, the flame propagating in the longitudinal and transverse directions at a speed of 30 mm/min, as shown in Figure 7a. Wood with a fire-retardant coating ignites in 45 s; however, the flame extinguishes automatically in 10 s after the gas burner is removed, as shown in Figure 7b.

When a sample with a coating applied only to a part of its surface is set on fire, the wood ignites from the uncoated side in 15 s. When the flame comes into contact with the coating, the coating gets foamed, and the flame extinguishes, as shown in Figure 8.

Thus, the possibility of using the developed compositions as fire-resistant coatings for wood has been proven.

The addition of diorite into the epoxy composition leads to an increase not only in thermal resistance, but also to an increase in the thermal stability of the epoxy composite. The studies have shown that the addition of 50 parts by mass of diorite ensures 100% of its tensile strength index at a temperature up to 75 °C, while an unfilled plasticized composite loses about 25% of its tensile strength, as shown in Figure 9.

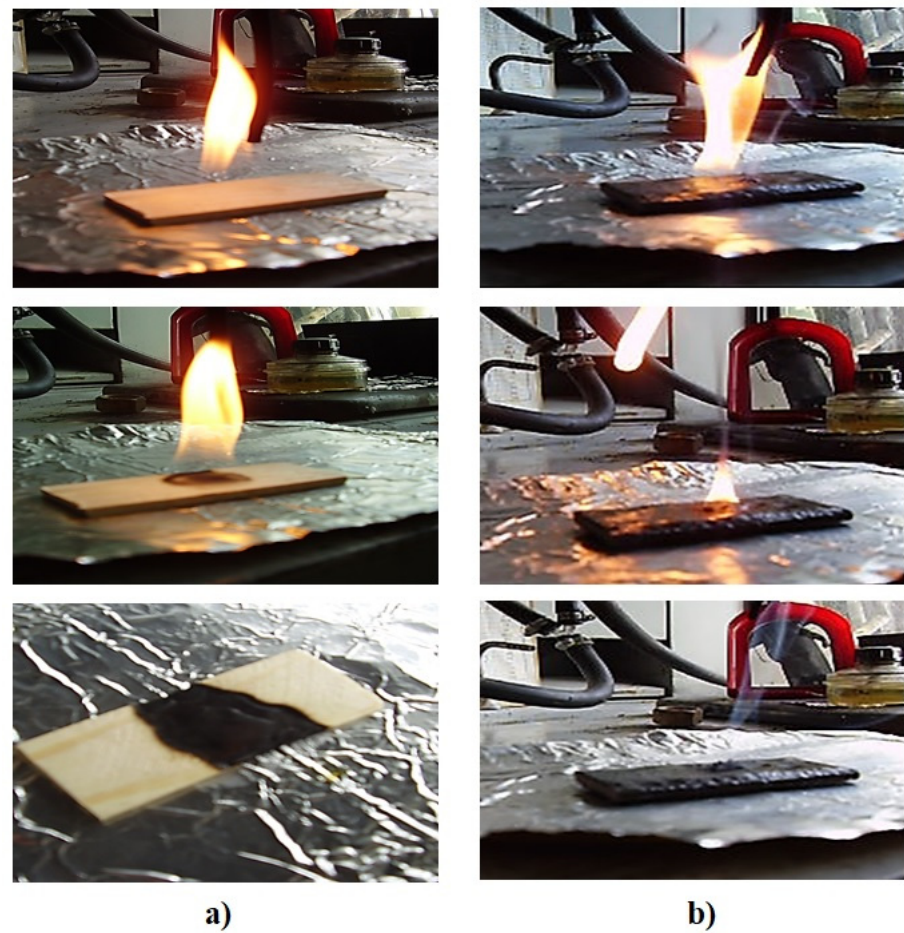


Figure 7. Flame propagation over the wood surface without a fire-resistant coating (a) and flame propagation over the wood surface with a fire-resistant coating (b).



Figure 8. Flame propagation over the surface of a sample with a flame-resistant coating applied only to a part of its surface.

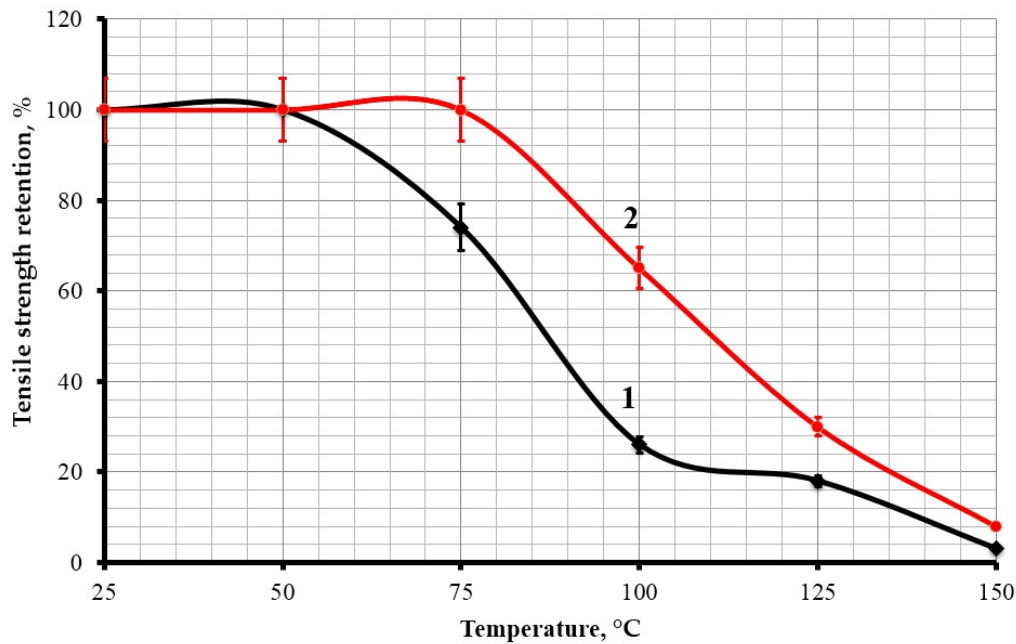


Figure 9. Dependences of the tensile strength index of the epoxy composite on the test temperature: 1—100ED-20 + 40ORPP + 15PEPA; 2—100ED-20 + 40ORPP + 50Diorite + 15PEPA.

To reduce the tendency to aggregate and to increase the adhesion capacity of diorite, it is necessary to functionalize it, which should ensure an effective adhesive interaction at the polymer matrix/filler interface. One of the promising methods of functionalization is the surface treatment of fillers with compounds that provide chemical interaction between the filler and the polymer matrix and reduce polydispersity of the filler, which will enhance the physical and mechanical properties of composites based on them [22,31–34]. APTES was used as such a compound.

The APTES treatment of the diorite surface changes its fractional composition. An increase in the number of particles with smaller sizes is observed, as shown in Figure 10, as is an increase in the specific surface area of diorite particles from 5.6 to 9.8 m²/g.

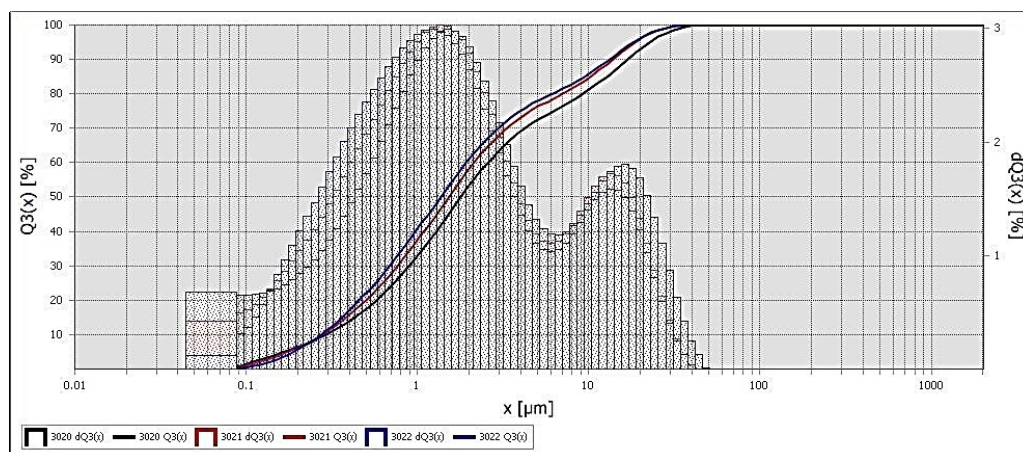


Figure 10. Fractional composition of diorite treated with APTES.

The presence of the interaction between the APTES amine groups and the ED-20 epoxy groups was proved earlier [22]. After the APTES treatment of the diorite surface, there appear vibration peaks corresponding to APTES in the IR spectra of functionalized diorite, as shown in Figure 11. Besides, a peak appears at 1040 cm⁻¹, which is connected

with the formation of a non-hydrolysable -Si-O-Si- bond, which remains after washing the functionalized diorite with water, thus confirming the chemical interaction between the functional groups of APTES and diorite.

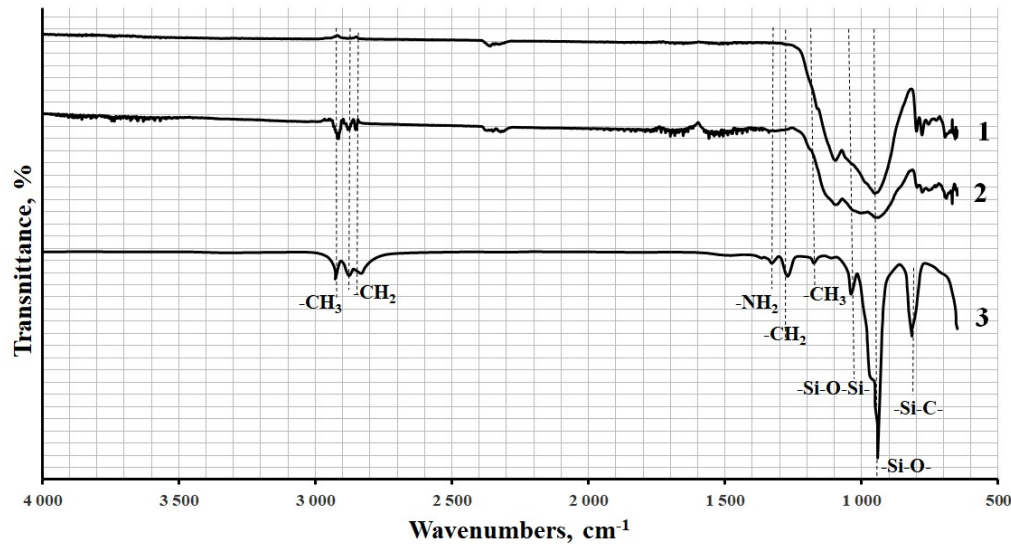


Figure 11. After the APTES treatment of the diorite surface, there appear vibration peaks corresponding to APTES in the IR spectra of functionalized diorite.

The addition of APTES-treated diorite into the epoxy composition accelerates the curing process, which can be seen in the reduction of the duration of the gelation process from 29 to 19 min, and the duration of the curing process from 40 to 28 min, with an increase in the maximum curing temperature from 116 to 122 °C, as shown in Table 5, in comparison with a composition containing original diorite, which further confirms the participation of APTES functional groups in the curing process.

The organization of chemical interaction at the polymer matrix/filler interface ensures an increase in the physicomechanical properties of epoxy composites. The addition of APTES-treated diorite into the epoxy composition increases all the studied strength properties by 11–48% as compared to the epoxy composite containing the original diorite, as shown in Figure 12.

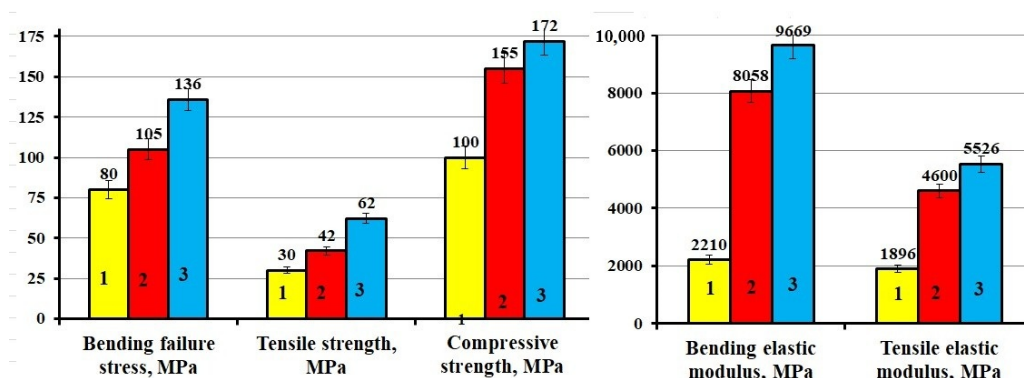


Figure 12. Physicomechanical characteristics of epoxy composites: 1—100 ED-20 + 40 ORPP + 15 PEPA; 2—100 ED-20 + 40 ORPP + 50 Diorite + 15 PEPA; 3—100 ED-20 + 40 ORPP + 50 Diorite_(APTES) + 15 PEPA.

Comparison of the developed compositions with existing analogues showed their competitiveness. The developed composites have physicomechanical characteristics comparable to those of the existing analogues and in some cases exceeding them, as shown in Table 8.

Table 8. Comparison of the developed materials with analogues.

Composition	σ_{ben} , MPa	E_{ben} , MPa	σ_{com} , MPa	σ_{ten} , MPa	E_{ten} , MPa
ED-20 + ORPP + PEPA + Diorite _(APTES)	136	9669	172	62	5526
	Analogues				
Epoxy resin + TETA + Fly ash [16]	-	-	160	48	-
DER-331 + JOINTMINE 905-3s + MMT [18]	-	-	-	50	1500
ED-20 + ORPP + PEPA + Ocher [7]	102	10,163	156	45	4110
ED-20 + PEPA + UDD [4]	102	3200	-	-	-
Epoxy resin + TETA + Granite _(TEMS) [19]	79	5126	107	-	-

Note: σ_{ben} —bending stress; E_{ben} —modulus of elasticity in bending; σ_{com} —compressive strength; σ_{ten} —tensile strength; E_{ten} —tensile modulus of elasticity; TETA—triethylenetetramine; DER-331—diglycidyl ether of bisphenol-A epoxy resin; JOINTMINE 905-3s—modified cycloaliphatic amine hardener; MMT—bi-functionalized montmorillonite; UDD—ultra-dispersed diamond; TEMS—triethoxymethylsilane.

4. Conclusions

The addition of diorite into the epoxy composition initiates the structure formation processes of an epoxy composite, which is observed in a reduction in the gelation time and the curing time (for a composition with a diorite content of 0.1 parts by mass), wherein the curing time for a composition with a diorite content of 50 parts by mass increases slightly, which is apparently due to the high viscosity of the composition and the steric hindrances of the curing process. Besides, the addition of diorite into the epoxy composition provides an increase in the curing degree of the epoxy composite, which allows the assumption that the diorite particles are additional cross-linking centers.

The addition of diorite into the epoxy composite ensures an increase in the heat resistance, thermal resistance and thermal stability of the composite. The thermal destruction of the epoxy composite containing diorite increases the yield of carbonized structures that prevent the release of volatile pyrolysis products into the gas phase, which reduces the flammability of the epoxy composite. The developed compositions filled with diorite do not support combustion in air and belong to the class of hardly flammable materials.

The efficiency of APTES-functionalization of the diorite surface has been proved, which provides chemical interaction at the polymer matrix/filler interface, and also prevents the aggregation of diorite particles, which, in general, ensures an enhancement of the strength characteristics of epoxy composite materials.

Author Contributions: Conceptualization, A.B., A.M., Y.K., M.A. and L.T.; Data curation, A.B., M.A. and L.T.; Formal analysis, A.B., Y.K., M.A. and L.T.; Funding acquisition, A.B.; Investigation, A.M.; Methodology, A.M. and Y.K.; Project administration, A.M.; Resources, Y.K.; Validation, A.M. and M.L.; Visualization, A.B., M.A., L.T. and M.L.; Writing—original draft, A.M.; Writing—review & editing, A.B., A.M., Y.K., M.A., L.T. and M.L. All authors have read and agreed to the published version of the manuscript.

Funding: This research has been funded by the Science Committee of Ministry of Education and Science of the Republic of Kazakhstan (Grant No. AP08955736).

Institutional Review Board Statement: Not applicable.

Informed Consent Statement: Not applicable.

Data Availability Statement: The data presented in this study are available on request from the corresponding author.

Conflicts of Interest: The authors declare no conflict of interest.

References

- Starokadomskii, D.L. Epoxy composites with 10 and 50 wt% micronanoiron: Strength, microstructure, and chemical and thermal resistance. *Russ. J. Appl. Chem.* **2017**, *90*, 1337–1345. [\[CrossRef\]](#)
- Buketov, A.V.; Sapronov, A.A.; Buketova, N.N.; Brailo, M.V.; Marushak, P.O.; Panin, S.V.; Amelin, M.Y. Impact toughness of nanocomposite materials filled with fullerene C60 particles. *Compos. Mech. Comput. Appl.* **2018**, *9*, 141–161. [\[CrossRef\]](#)
- Mostovoi, A.S.; Plakunova, E.V.; Panova, L.G. New Epoxy Composites Based on Potassium Polytitanates. *Int. Polym. Sci. Technol.* **2013**, *40*, 49–51. [\[CrossRef\]](#)

4. Buketov, A.V.; Saprionov, O.O.; Brailo, M.V.; Maruschak, P.O.; Yakushchenko, S.V.; Panin, S.V.; Nigalatiy, V.D. Dynamics of destruction of epoxy composites filled with ultra-dispersed diamond under impact conditions. *Mech. Adv. Mater. Struct.* **2020**, *27*, 725–733. [[CrossRef](#)]
5. Hu, J.H.; Shan, J.Y.; Wen, D.H.; Liu, X.X.; Zhao, J.Q.; Tong, Z. Flame retardant, mechanical properties and curing kinetics of DOPO-based epoxy resins. *Polym. Degrad. Stab.* **2014**, *109*, 218–225. [[CrossRef](#)]
6. Mostovoy, A.S.; Nurtazina, A.S.; Burmistrov, I.N.; Kadykova, Y.A. Effect of Finely Dispersed Chromite on the Physicochemical and Mechanical Properties of Modified Epoxy Composites. *Russ. J. Appl. Chem.* **2018**, *91*, 1758–1766. [[CrossRef](#)]
7. Bekeshev, A.; Mostovoy, A.; Tastanova, L.; Kadykova, Y.; Kalganova, S.; Lopukhova, M. Reinforcement of Epoxy Composites with Application of Finely-ground Ochre and Electrophysical Method of the Composition Modification. *Polymers* **2020**, *12*, 1437. [[CrossRef](#)]
8. Pati, P.R.; Satpathy, M.P. Investigation on red brick dust filled epoxy composites using ant lion optimization approach. *Polym. Compos.* **2019**, *40*, 3877–3885. [[CrossRef](#)]
9. Kumara, R.; Kumarb, K.; Sahooc, P.; Bhowmika, S. Study of mechanical properties of wood dust reinforced epoxy composite. *Procedia Mater. Sci.* **2014**, *6*, 551–556. [[CrossRef](#)]
10. Behzadnasab, M.; Mirabedini, S.M.; Esfandeh, M. Corrosion protection of steel by epoxy nanocomposite coatings containing various combinations of clay and nanoparticulate zirconia. *Corros. Sci.* **2013**, *75*, 134–141. [[CrossRef](#)]
11. Syugaev, A.V.; Maratkanova, A.N.; Shakov, A.A.; Nelyubov, A.V.; Lomayeva, S.F. Surface modification of iron particles with polystyrene and surfactants under high-energy ball milling. *Surf. Coat. Technol.* **2013**, *236*, 429–437. [[CrossRef](#)]
12. Vahedi, H.; Pasbakhsh, P. Instrumented impact properties and fracture behaviour of epoxy/modified halloysitenanocomposites. *Polym. Test.* **2014**, *39*, 101–114. [[CrossRef](#)]
13. Mostovoi, A.S.; Kurbatova, E.A. Controlling the properties of epoxy composites filled with brick dust. *Russ. J. Appl. Chem.* **2017**, *90*, 267–276. [[CrossRef](#)]
14. Karnati, S.R.; Agbo, P.; Zhang, L. Applications of silica nanoparticles in glass/carbon fiber-reinforced epoxy nanocomposite. *Compos. Commun.* **2020**, *17*, 32–41. [[CrossRef](#)]
15. Clifton, S.; Thimmappa, B.H.S.; Selvam, R.; Shivamurthy, B. Polymer nanocomposites for high-velocity impact applications—A review. *Compos. Commun.* **2020**, *17*, 72–86. [[CrossRef](#)]
16. Sim, J.; Kang, Y.; Kim, B.J.; Park, Y.H.; Lee, Y.C. Preparation of Fly Ash/Epoxy Composites and Its Effects on Mechanical Properties. *Polymers* **2020**, *12*, 79. [[CrossRef](#)]
17. Kulkarni, S.M. Kishore Effect of filler-fiber interactions on compressive strength of fly ash and short-fiber epoxy composites. *J. Appl. Polym. Sci.* **2003**, *87*, 836–841. [[CrossRef](#)]
18. Sand Chee, S.; Jawaid, M. The Effect of Bi-Functionalized MMT on Morphology, Thermal Stability, Dynamic Mechanical, and Tensile Properties of Epoxy/Organoclay Nanocomposites. *Polymers* **2019**, *11*, 2012. [[CrossRef](#)]
19. Ramakrishna, H.V.; Priya, S.P.; Rai, S.K. Flexural, compression, chemical resistance, and morphology studies on granite powder-filled epoxy and acrylonitrile butadiene styrene-toughened epoxy matrices. *J. Appl. Polym. Sci.* **2007**, *104*, 171–177. [[CrossRef](#)]
20. Mostovoy, A.S.; Nurtazina, A.S.; Kadykova, Y.A.; Bekeshev, A.Z. Highly Efficient Plasticizers-Antipirenes for Epoxy Polymers. *Inorg. Mater. Appl. Res.* **2019**, *10*, 1135–1139. [[CrossRef](#)]
21. Fang, F.; Huo, S.; Shen, H.; Ran, S.; Wang, H.; Song, P.; Fang, Z. A bio-based ionic complex with different oxidation states of phosphorus for reducing flammability and smoke release of epoxy resins. *Compos. Commun.* **2020**, *17*, 104–108. [[CrossRef](#)]
22. Mostovoy, A.S.; Vikulova, M.A.; Lopukhova, M.I. Reinforcing effects of aminosilane-functionalized h-BN on the physico-chemical and mechanical behaviors of epoxy nanocomposites. *Sci. Rep.* **2020**, *10*, 10676. [[CrossRef](#)] [[PubMed](#)]
23. Tikhani, F.; Moghari, S.; Jouyandeh, M.; Laoutid, F.; Vahabi, H.; Saeb, M.R.; Dubois, P. Curing Kinetics and Thermal Stability of Epoxy Composites Containing Newly Obtained Nano-Scale Aluminum Hypophosphite (AlPO₂). *Polymers* **2020**, *12*, 644. [[CrossRef](#)] [[PubMed](#)]
24. Hameed, A.; Islam, M.; Ahmad, I.; Mahmood, N.; Saeed, S.; Javed, H. Thermal and mechanical properties of carbon nanotube/epoxy nanocomposites reinforced with pristine and functionalized multiwalled carbon nanotubes. *Polym. Compos.* **2015**, *36*, 1891–1898. [[CrossRef](#)]
25. Sul, J.-H.; Prusty, B.G.; Crosky, A. Effect of the addition of multi-walled carbon nanotubes on the thermomechanical properties of epoxy resin. *Polym. Compos.* **2017**, *38*, 1873–1880. [[CrossRef](#)]
26. Choi, W.J.; Powell, R.L.; Kim, D.S. Curing behavior and properties of epoxy nanocomposites with amine functionalized multi-walled carbon nanotubes. *Polym. Compos.* **2009**, *30*, 415–421. [[CrossRef](#)]
27. Rajaram, A.N.; Boay, C.G.; Srikanth, N. Effect of curing on the hygrothermal behaviour of epoxy and its carbon composite material. *Compos. Commun.* **2020**, *22*, 100507. [[CrossRef](#)]
28. Qian, L.; Qiu, Y.; Sun, N.; Xu, M.; Xu, G.; Xin, F.; Chen, Y. Pyrolysis route of a novel flame retardant constructed by phosphaphenanthrene and triazine-trione groups and its flame-retardant effect on epoxy resin. *Polym. Degrad. Stab.* **2014**, *107*, 98–105. [[CrossRef](#)]
29. Li, W.; Song, B.; Zhang, S.; Zhang, F.; Liu, C.; Zhang, N.; Yao, H.; Shi, Y. Using 3-Isocyanatopropyltrimethoxysilane to Decorate Graphene Oxide with Nano-Titanium Dioxide for Enhancing the Anti-Corrosion Properties of Epoxy Coating. *Polymers* **2020**, *12*, 837. [[CrossRef](#)]

30. Buketov, A.V.; Dolgov, N.A.; Sapronov, A.A.; Nigalatii, V.D.; Babich, N.V. Mechanical Characteristics of Epoxy Nanocomposite Coatings with Ultradisperse Diamond Particles. *Strength Mater.* **2017**, *49*, 464–471. [[CrossRef](#)]
31. Wong, T.-T.; Lau, K.-T.; Tam, W.-Y.; Etches, J.A.; Kim, J.-K.; Wu, Y. Effects of silane surfactant on Nano-ZnO and rheology properties of nano-ZnO/epoxy on the UV absorbability of nano-ZnO/epoxy/micron-HGF composite. *Compos. Part B* **2016**, *90*, 378–385. [[CrossRef](#)]
32. Lavorgna, M.; Romeo, V.; Martone, A.; Zarrelli, M.; Giordano, M.; Buonocore, G.G.; Qu, M.Z.; Fei, G.X.; Xia, H.S. Silanization and silica enrichment of multiwalled carbon nanotubes: Synergistic effects on the thermal-mechanical properties of epoxy nanocomposites. *Eur. Polym. J.* **2013**, *49*, 428–438. [[CrossRef](#)]
33. Shen, J.F.; Huang, W.S.; Wu, L.P.; Hu, Y.Z.; Ye, M.X. The reinforcement role of different amino-functionalized multi-walled carbon nanotubes in epoxy nanocomposites. *Compos. Sci. Technol.* **2007**, *67*, 3041–3050. [[CrossRef](#)]
34. Wang, M.; Ma, L.; Li, B.; Zhang, W.; Zheng, H.; Wu, G.; Huang, Y.; Song, G. One-step generation of silica particles onto graphene oxide sheets for superior mechanical properties of epoxy composite and scale application. *Compos. Commun.* **2020**, *22*, 100514. [[CrossRef](#)]